Advances in Science and Technology Research Journal

Advances in Science and Technology Research Journal, 2025, 19(7), 480–495
https://doi.org/10.12913/22998624/204303
ISSN 2299-8624, License CC-BY 4.0

Received: 2025.03.12
Accepted: 2025.04.23
Published: 2025.05.25

Investigation of effective parameters on oxygen free high conductivity copper deformation based on cutting molds design and numerical approach

Wael H.A. Shaheen[1*], M. Salman[1], Raghad Ahmed Alaloosi[1], Moneer H. Tolephih[2], Wassan S. Abd Al-Sahb[3], Oday I. Abdullah[4,5,6]

[1] Department of Automated Manufacturing Engineering, Al-Khwarizmi College of Engineering, University of Baghdad, Al-Jadryah, Baghdad, Iraq
[2] AlNaji University, Baghdad, Iraq
[3] Department of Mechanical Engineering, College of Engineering, University of Baghdad, Al-Jadryah, Baghdad, Iraq
[4] Department of Energy Engineering, College of Engineering, University of Baghdad, Al-Jadryah, Baghdad, Iraq
[5] College of Engineering, AlNaji University, Baghdad, Iraq
[6] Department of Mechanics, Al-Farabi Kazakh National University, Almaty 050040, Kazakhstan
* Corresponding author's e-mail: waelshaheen@kecbu.uobaghdad.edu.iq

ABSTRACT

This paper investigates the effect of using different values of selected parameters on directional deformations of the oxygen free high conductivity copper rectangular shape product. These parameters include cutting velocity, initial sheet temperature, and punch fillet radius. The article introduces a comprehensive study of cutting mold design procedures and analysis in terms of the directional deformation of the product. The deformations have been analyzed numerically to determine the highest and lowest values of the product utilizing analysis system (ANSYS) software 18.1. The analysis shows the rise in the deformation as the cutting velocity increases from 40 mm/s to 80 mm/s. Deformation is lowest at 0 °C and peaks at 80 °C. The smallest deformation with a punch fillet radius of 0.1 mm, while a 0.9 mm radius maximizes it. The deformation increases significantly when the velocity increases from 70 mm/s to 80 mm/s and fillet radii rise from 0.7 mm to 0.9 mm. The higher velocities above 60 mm/s and high temperatures over 60 °C result in greater product deformation. The significant rise in the deformation value occurs at temperatures above 60 °C and fillet radii above 0.7 mm, while the minimal value occurs at temperatures below 40 °C and fillet radii below 0.3 mm. Also, it showed that deformation increases by 30–40% at high cutting velocities, initial sheet temperatures, and fillet radii. The cutting mold model is validated by comparing the current numerical results with available published data for copper sheet blanking. The directional deformations of the present numerical modeling and the experimental work of the available literature appeared in a good agreement with an error value not exceeding the range of 1–3%.

Keywords: finite element method, directional deformation, cutting velocity, initial sheet temperature, punch fillet radius, cutting mold design.

INTRODUCTION

Through the recent years, the high cost production processes have been replaced by cost-effective methods such as cutting molds in the sheet metalworking industry [1]. This industry is based on material removal and is applicable to sheet materials with thickness ranging from 0.4 mm to 6 mm [2]. The cutting molds are multipurpose tools used for processing various sheet metals such as steel, aluminum, copper, and brass [3]. They can be utilized to manufacture various products with high cutting quality and accurate dimensions. These products can be used in many industries such as home devices, railway stations, automobiles spare parts, and aircrafts [4, 5]. The cutting mold can perform a single cutting operation including piercing or blanking to manufacture the required product [6]. The upper component of the cutting mold is called the punch, which is responsible for implementing the single blanking process for the metal in a vertical motion to produce the final product. The blanking process is initiated as the punch comes into contact with the top surface of the sheet metal, applying compressive force to penetrate the metal sheet and separating the required product [7].

Different researchers have studied the effect of selected cutting parameters on the deformation of products after completing the blanking or piercing process. However, there is no study about improving the product cutting quality based on minimum directional deformation. The product deformation is measured after completing the single-cutting operation using a cutting mold. Laxman and Mirza [8] used a developed mathematical model, design of experiments, and analysis of variance to predict optimum clearance for achieving high-quality copper products. The academic researchers investigated the influence of punch geometry and wear, punch-die clearance, and sheet material type with thickness on product cutting quality. They succeeded in predicting the optimum set of selected parameters for obtaining improved cutting quality of products. Gökçe [9] implemented the experimental, modelling, and optimizing aspects for studying the effect of using various variables on the drilling process of 450 martensitic stainless steel sheets without using coolant. These parameters include cutting force, temperature, cutting velocity, feed rate, and burr height. The results indicated that the increase in feed rate led to an increase in burr heights and cutting forces. Tushar and Vijay [10] were able to predict burr heights in sheet metal trimming operations using artificial neural networks and acoustic signals. The researchers studied the influence of cutting punch wear, clearance, and thickness of sheet metal on burr heights. The proposed methodology can be used for improving productivity, minimizing production defects, and decreasing inspection time. Mohamed et al. [11] utilized the fine blanking operation simulation of steel sheets to study the effect of burr heights, cutting edge shape, and dimensional accuracy on product quality and stress state of cutting steel sheets. The authors were able to estimate the distributions of both plastic strain and shear stress on the shearing zone through the cutting process. Shamik et al. [12] used ductile fracture modeling and finite element simulation for numerical prediction of burr heights, cutting edge profiles, and fracture initiation in the steel and aluminum sheets. The outcomes showed that the aluminum sheet burr heights are larger than steel sheet and the burr formations of aluminum are more effective in clearance compared to steel. Kamarul et al. [13] studied the influence of clearance parameters on burr heights of aluminum, brass, and mild steel sheets in blanking operations. The outcomes showed that the low clearance provides low burr heights for aluminum sheets. While the high clearance provides high burr formations for brass and mild steel sheet. Hüseyin et al. [14] analyzed, modeled, and optimized burr heights during laser drilling and cutting of ferritic stainless steel. They studied the effect of focal point, gas pressure, and cutting velocity on cutting operation efficiency, product quality, and production rate. The authors found that the cutting velocity is the most effective variable on burr formations compared with other variables. Ashutosh and Anand [15] conducted the simulation and experimental analysis to investigate the effect of geometry angle variation, punch cutting edge radius, and clearance on rollover depth after cutting the sheet material. The outcomes showed that the rollover depth increases when the blank geometry angle and punch edge radius decrease. Farshid et al. [16] used the experimental aspect to study the influence of sheet metal thickness clearance percentage on rollover zone, fracture zone, shear zone, fracture angle, and burr heights. The outcomes indicated that the clearance percentage from (9–15) provides thick rollover and fracture, and a thin shear zone. In addition, the clearance percentage from (15–21) provides low rollover thickness, fracture, and shear zones. While the clearance percentage from (9–21) provides an increase in fracture angle and burr heights. Anna et al. [17] used the drilling simulation process of aluminum sheets to obtain a new burr model that can be used to predict the drilling burr thicknesses and heights which affect tool wear. The results showed that the burr height and thickness increase when tool wear increases. Kaan [18] utilized finite element analysis and Deform software to study the effect of using different notch angles and depths on the cutting operation of stainless steel sheets. He investigated experimentally the effect of shear zone distributions on product surface quality, cutting forces, and crack angles. The author obtained better cutting surface quality and he found that notch depth and angle have significant effects on cutting force. Fenghe et al. [19] applied the finite element method to simulate the cutting process, measure burr heights, and create a new burr theoretical model. The authors investigated experimentally the influence of using various exit surface angles on burr heights of aluminum sheets. They obtain the relationship between bending point position and burr height shape. Mohammad and Salman [20] used finite element analysis to study the influence of punch tool wear on tool life. They found that the tool wear increases when the cutting edge of the punch increases. Furthermore, the punch wear reduces when the sheet metal deformation increases. Many other studies employed different methods to investigate the effect of cutting parameters on product quality and materials behavior. These methods include Taguchi method, analysis of variance, and multiscale modelling approach. They can be used to estimate the effect of nanocomposites inclusion on the overall thermomechanical properties of the studied materials, and to determine the most effective parameter on final product quality [21–23].

The previous studies lacked detailed information about the properties of the metal used in manufacturing cutting mold components, the dimensional details of products, standard design calculations, product directional deformations, and the associated manufacturing cost. As for the reviewed literature, there is a need for a complete study of the effect of cutting velocity, initial sheet temperature, and punch fillet radius on product cutting quality. Therefore, the current article concentrates on investigating the influence of using different values for velocity, temperature, and fillet radius on the rectangular shape product cutting quality. The selected parameters can contribute to improving the cutting mold efficiency for achieving a single cutting process for manufacturing the product. The study attempts to develop the cutting mold performance and obtain a better quality of the product. The numerical analyses in this article will determine which variable has a more important effect on product quality compared with other variables. The outcomes of this research can contribute to better-cutting mold design and reduce the cost of product and mold.

CUTTING MOLD DESIGN

The design procedure of cutting mold models was achieved using manufacturing standards and mathematical equations related to the mold design. The proposed mold models can be used to manufacture a metal rectangular shape product. The dimensions and shape of product are selected from internet data source as shown in Figure 1 [24].

The oxygen free high conductivity copper was selected as the product metal. It has uniform temperature and different properties which are presented in Table 1 [25].

The required cutting force value to implement the cutting process by the punch for obtaining the final product was calculated using Equation 1. [26]. The computed cutting force is equal to 85170 N.

$$Cutting\ force = Cut\ perimeter\ \times \\ \times\ Sheet\ thickness\ \times\ Shear\ strength \tag{1}$$

The product orientation on sheet material is selected based on design requirements. When the thickness of the sheet is more than 0.6 mm, the D_H amount is selected from Table 2 and the D_V(vertical dimension between two edges including sheet material and product, mm) amount is obtained from Equation 2. [27].

$$D_V = T_{SM} + 0.015\ H_P \tag{2}$$

There are two options for product arrangement on sheet material including horizontal and vertical position. The horizontal represents the best option as it provides the highest percentage of used metal under the lowest scrap material. The P_{SMU} (sheet material utilization percentage, %) is computed by utilizing Equation 3. [28].

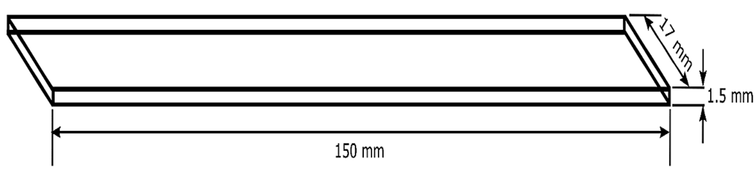

Figure 1. Dimensions of rectangular shape product

Table 1. Properties of CU-OFHC

Property	Value	Unit
Density	8940	kg/m^3
Ultimate tensile strength	260	MPa
Yield tensile strength	205	MPa
Modulus of elasticity	115	MPa
Poisson's ratio	0.31	/
Shear modulus	44	GPa
Shear strength	170	MPa
Specific heat	385	JKg-1C-1

Table 2. Absolute values of D_H

Dimension (mm)	T_{SM} > 0.6 mm				
	0.61 to 0.8	0.81 to 1.25	1.26 to 2.5	2.51 to 4	4.1 to 6
D_H	3.5	4.3	5.5	6	7

$$P_{SMU} = \left[\frac{A_P}{(W_P+D_H)\, W_S}\right] \times 100 \tag{3}$$

The total clearance between punch and mold is considered an important variable that has a high influence on product deformation. The calculated clearance value is equal to 0.09 mm based on using Equation 4. [29]. The details of cutting punch dimensions are presented in Table 3. Five different punch fillet radii have been selected in this research for obtaining the rectangular-shaped product. These punch fillet radii include 0.1, 0.3, 0.5, 0.7, and 0.9 mm.

$$Clearance = (4-8)\% \times \times Sheet\ metal\ thickness \tag{4}$$

The mold block dimensions are selected in this study based on design requirements. The dimensions of the mold block are calculated using Equations 5, 6, 7, and 8. [30]. The C value was selected equal to 0.9 from Table 4 [30] based on the ultimate tensile strength of CU-OFHC (oxygen free high conductivity copper) which is equal to 250 MPa. The details of the mold block are shown in Table 5. The three-dimensional completed cutting mold is shown in Figure 2.

$$T_{MB} = \left(10 + 5\,T_{SM} + 0.7\sqrt{L_{MBO} + H_{MBO}}\right) \times C \tag{5}$$

$$D = (10\ to\ 12) + 0.8\,T_{MB} \tag{6}$$

$$L_{MB} = L_{MBO} + 2D \tag{7}$$

$$H_{MB} = H_{MBO} + 2D \tag{8}$$

Table 3. Dimensions of cutting punch

Punch elements	Dimension in mm	
	Punch shoulder	Punch
Length	155	55
Width	22	16.91
Height	5	149.91

COMPUTATIONAL MODELING AND ANALYSIS

The explicit dynamics used for simulation and modeling instead of implicit approach because it provides high accurate numerical results for problems having nonlinear dynamic, large deformation, contact impact, multi-body contact, and nonlinear material behavior. The temperature independent material properties are used in the analysis stage for copper sheet, cutting punch, and mold block. The first step of numerical methodology was to enter the selected values into the engineering data section of the explicit dynamics of ANSYS (analysis system) software. These values represented the properties of the cutting punch, mold block, and oxygen free high conductivity copper sheet. The properties of the rectangular-shaped product sheet are presented in Table 1. In this research, it has been selected tool steel S7 a metal for cutting punch and mold

Table 4. Values of C and ultimate tensile strength of sheet metal

Ultimate tensile strength (MPa)	117	245	392	784
C	0.6	0.8	1	1.3

Table 5. Dimensions of mold block

Mold block elements	Dimension in mm
L_{MBO}	150
L_{MB}	210
H_{MBO}	17
H_{MB}	77
T_{MB}	25
D	30

block. The properties of this metal are taken from ANSYS data as indicated in Table 6. The engineering and true stress-strain curves of steel S7 are shown in Figure 3 [31]. The non-linear finite element analyses were performed for materials (CU-OFHC and steel S7) and geometric shape of cutting mold parts (cutting punch, mold block, and sheet metal).

The three-dimensional models of cutting mold parts including cutting punch, mold block, and copper sheet metal are drawn using ANSYS to complete the geometry field. The manual contacts between cutting mold parts were applied to obtain accurate numerical results. The bonded solid to solid option was implemented on mold block and copper sheet. The frictional solid to solid option was implemented on cutting punch and copper sheet using friction coefficient of 0.3. The three-dimensional elements of hexahedron and triangular prism were used for meshing of copper sheet and (cutting punch and mold block) respectively. A hexahedron element has eight vertices (nodes), twelve edges, six quadrilateral faces, and three degrees of freedom per node. A triangular prism element has six vertices (nodes), nine edges, two triangular, three quadrilateral faces, and three degrees of freedom per node. The meshing stage has a significant effect on the final outcomes; therefore, the convergence method has been applied to verify the selected mesh. Different methods including an average of skewness orthogonal quality, and h-convergence are applied to improve the mesh efficiency and quality as shown in Figure 4. The average values of skewness and orthogonal quality are 0.03 and 0.96 respectively. Both values are considered excellent compared with mesh metrics spectrum values as shown in Table 7 [32].

The mesh size has a significant effect on data analysis time to obtain the final results. The fine mesh led to an increase in the solution time and provided accurate outcomes. While the coarse mesh led to reduced solution time and obtained non-accurate results. The authors of this article were enabled to make a balance between the output data accuracy (results) and the mesh element size. This balance can minimize both the computer use cost and the required time to obtain the results. Different mesh sizes including 0.16 mm, 0.5 mm, and 0.8 mm were applied on the sheet metal body, cutting face of the punch, and upper face of the

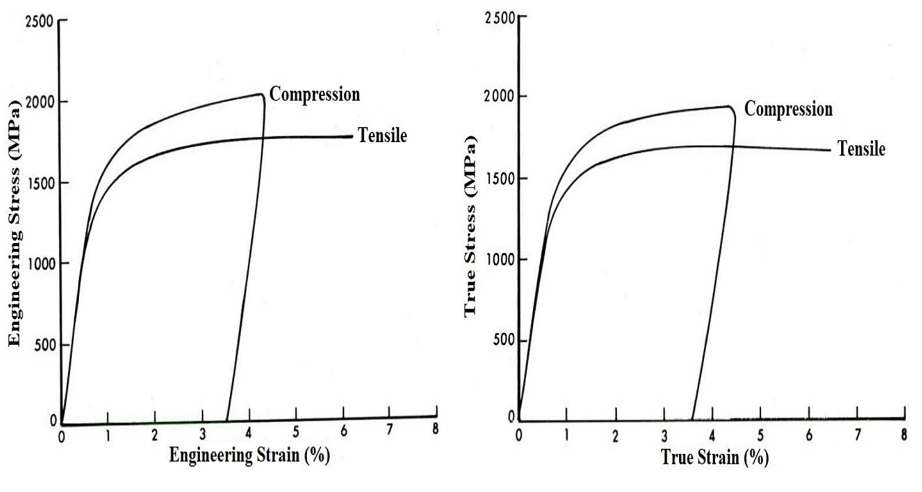

Figure 2. Three-dimensional completed cutting mold

Table 6. Material properties of cutting mold parts

Properties of steel S7	Unit	Cutting punch	Mold block
Density	Kg/m^3	7750	7750
Specific heat	$JKg^{-1}C^{-1}$	477	477
Initial yield stress	MPa	1539	1539
Hardening constant	MPa	477	477
Shear modulus	GPa	81800	81800

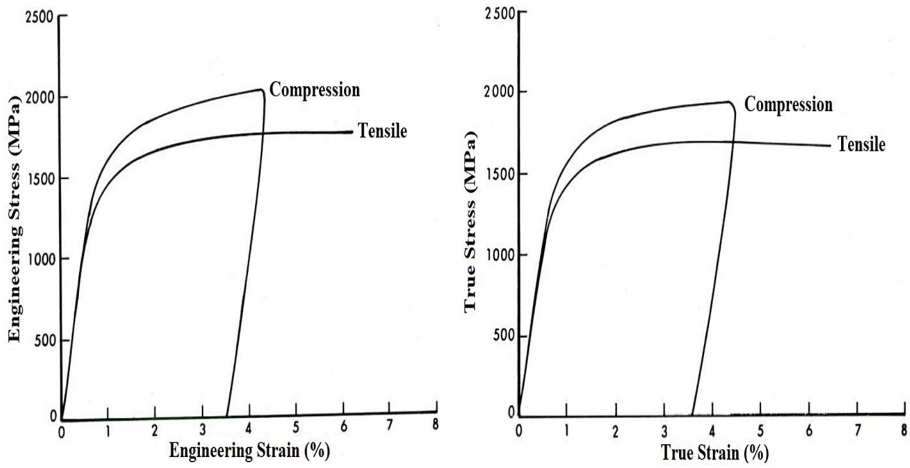

Figure 3. Engineering and true stress-strain curve of steel S7

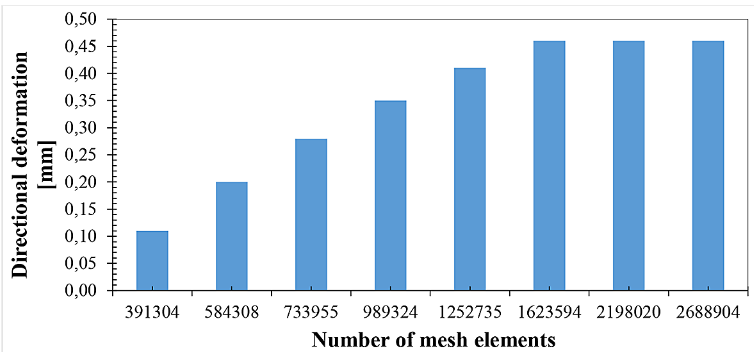

Figure 4. H-convergence for mesh quality of cutting mold and sheet metal

mold respectively. The three-dimensional mesh of full cutting mold is shown in Figure 5.

The high density of mesh was utilized at the sheet metal cutting zone as this zone has large deformation levels. The low density of mesh was used at other regions far from the cutting zone as these regions have small deformation levels. The boundary conditions including cutting force, cutting velocity, fixed supports, and analysis settings are applied to cutting mold models. The locations of cutting force and velocity are selected on the top part of the cutting punch as shown in Figures 6–7. The fixed supports option was applied on the mold block as shown in Figure 8. The analysis settings that are applied to cutting mold models in the finite element model are shown in Figure 9. Different values of parameters including cutting velocity, initial sheet temperature, and punch fillet radius were selected to determine the better values for these parameters under the lowest directional deformations for rectangular shape products. These values are (40, 50, 60, 70, and 80) mm/s for velocity, (0, 20, 40, 60, and 80) °C for temperature, and (0.1, 0.3, 0.5, 0.7, and 0.9) mm for fillet radius. Some values of parameters are selected based on previous papers in the field of metal cutting operations

Table 7. Mesh metrics spectrum for average values of skewness and orthogonal quality

Average skewness					
Unacceptable	Bad	Acceptable	Good	Very good	Excellent
0.98–1.00	0.95–0.97	0.80–0.94	0.50–0.80	0.25–0.50	0–0.25
Average orthogonal quality					
Unacceptable	Bad	Acceptable	Good	Very good	Excellent
0–0.001	0.001–0.14	0.15–0.20	0.20–0.69	0.70–0.95	0.95–1.00

and other values are chosen randomly to check the effect of each value on directional deformations of the copper product. The full combination between values of parameters provides 125 cases for all possibilities and these cases are investigated in this study. The dynamic simulation stage starts when the cutting punch moves toward the mold block for contacting the copper sheet which exists on the upper face of the mold. Then, the punch is applied continuous pressure on the sheet to penetrate it and to separate the copper product. The ANSYS simulation of single blanking operation by the cutting mold provides outcomes including directional deformations of the product. Various stages as shown in Figure 10 were applied to achieve the numerical simulation aspect for obtaining accurate results in terms of product deformations.

MODAL VALIDATION

The cutting mold model is validated by comparing the present numerical results with the experimental outcomes of Vaditake and Shinde [33] for copper sheet blanking. Figure 11 (a, b, and c) shows comparisons of directional deformations

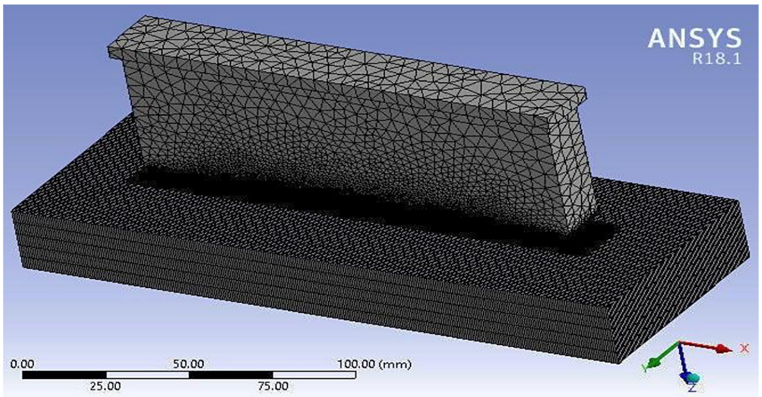

Figure 5. Three-dimensional mesh of full-cutting mold

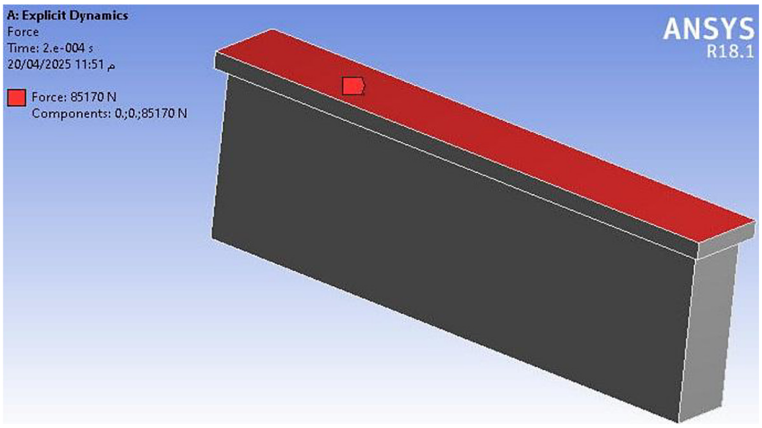

Figure 6. Cutting force location on cutting punch

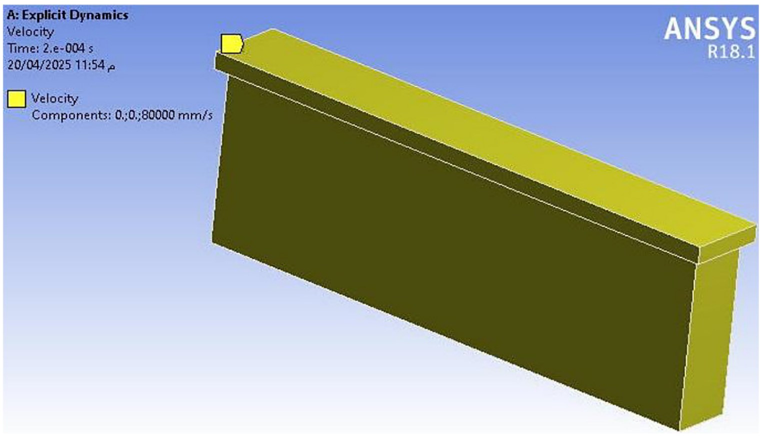

Figure 7. Cutting velocity location on cutting punch

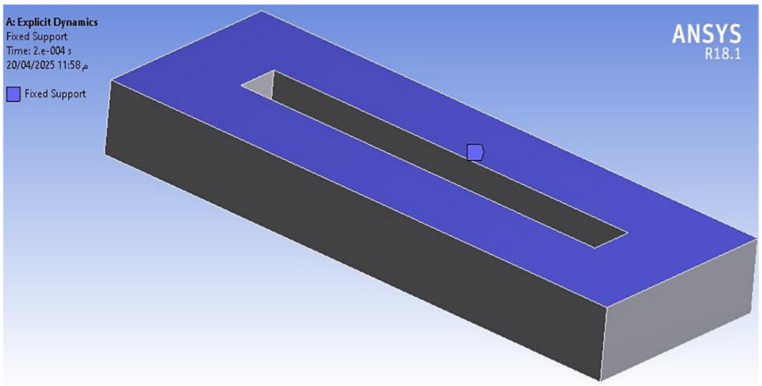

Figure 8. Fixed support location on mold block

Details of "Analysis Settings"

Analysis Settings Preference	
Type	Program Controlled
Step Controls	
Resume From Cycle	0
Maximum Number of Cycles	1e+07
End Time	2.e-004 s
Maximum Energy Error	0.1
Reference Energy Cycle	0
Initial Time Step	Program Controlled
Minimum Time Step	Program Controlled
Maximum Time Step	Program Controlled
Time Step Safety Factor	0.9
Characteristic Dimension	Diagonals
Automatic Mass Scaling	No
Solver Controls	
Solve Units	mm, mg, ms
Beam Solution Type	Bending
Beam Time Step Safety Factor	0.5
Hex Integration Type	Exact
Shell Sublayers	3
Shell Shear Correction Factor	0.8333
Shell BWC Warp Correction	Yes
Shell Thickness Update	Nodal
Tet Integration	Average Nodal Pressure
Shell Inertia Update	Recompute
Density Update	Program Controlled
Minimum Velocity	1.e-003 mm s^-1

Details of "Analysis Settings"

Maximum Velocity	1.e+013 mm s^-1
Radius Cutoff	1.e-003
Minimum Strain Rate Cutoff	1.e-010
Euler Domain Controls	
Domain Size Definition	Program Controlled
Display Euler Domain	Yes
Scope	All Bodies
X Scale factor	1.2
Y Scale factor	1.2
Z Scale factor	1.2
Domain Resolution Definition	Total Cells
Total Cells	2.5e+05
Lower X Face	Flow Out
Lower Y Face	Flow Out
Lower Z Face	Flow Out
Upper X Face	Flow Out
Upper Y Face	Flow Out
Upper Z Face	Flow Out
Euler Tracking	By Body
Damping Controls	
Linear Artificial Viscosity	0.2
Quadratic Artificial Viscosity	1.
Linear Viscosity in Expansion	No
Artificial Viscosity For Shells	Yes
Hourglass Damping	AUTODYN Standard
Viscous Coefficient	0.1
Static Damping	0.

Figure 9. Details of analysis settings

of the rectangular shape product at ranges of sheet metal thickness, clearance, and punch wear radius. The cutting velocity and temperature of both simulation and experimental aspects are assumed to be similar for validation and comparison aspects. The experimental values of selected parameters are applied to some models of cutting mold in the present work. Figure 11 shows good agreement between the values of the directional deformations for the present numerical modeling and the experimental work in the literature with an error value not exceeding the range of 1–3%.

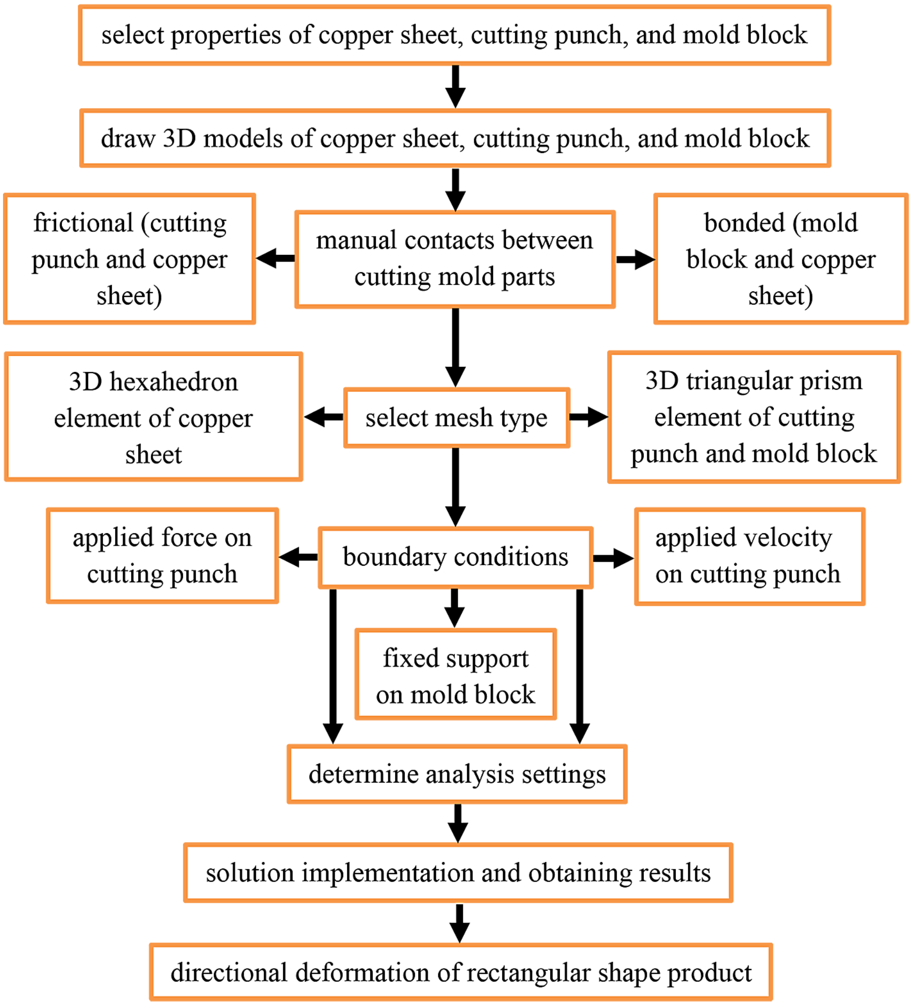

Figure 10. Modelling and simulation stages of cutting mold and blanking process

RESULTS

The ANSYS software is used to obtain output data of directional deformations of the rectangular shape product based on applying different values of input data of selected parameters. The variables are cutting velocity, initial sheet temperature, and punch fillet radius. The product deformations are applied as criteria to determine the cutting quality. Different velocities of 40, 50, 60, 70, and 80 mm/s, temperatures of 0, 20, 40, 60, and 80 °C, and fillet radii of 0.1, 0.3, 0.5, 0.7, and 0.9 mm are selected in this research. The accurate results in terms of product deformations were obtained by using suitable metals and properties for cutting mold parts, improved quality of the mesh, correct boundary conditions, and manual contacts between mold parts. The different values of oxygen free high conductivity copper product deformation were obtained utilizing various cutting mold models and selected parameters. These models are built based on different cutting punch fillet radii. The best punch fillet radius was achieved depending on the lowest directional deformation of the final product. The cutting punch models should be traveled to a safe distance inside the sheet material as shown in Figure 12 to complete the single blanking process for obtaining correct and accurate values of deformations.

The investigation process of directional deformations indicated that the high cutting velocities, initial sheet temperatures, and punch fillet radii led to an increase in the deformation amounts. While, the defamations decrease when applying low velocities, temperatures, and fillet radii. The results show different deformations of the rectangular shape product after completing the cutting operation because of applying various input data of selected parameters. The best

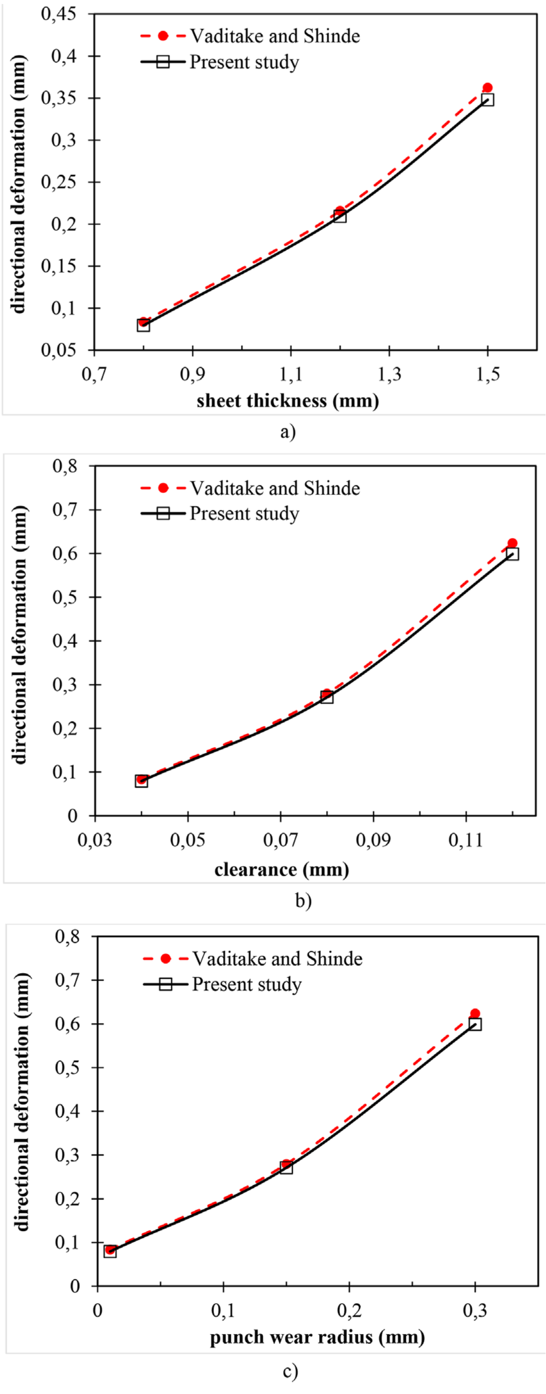

Figure 11. Comparison between present work and Vaditake and Shinde for directional deformation at ranges of: (a) sheet thickness, (b) clearance, and (c) punch wear radius

cutting mold model was selected based on the minimum directional deformation of the product as shown in Figure 13.

The following sections will discuss in detail the effect of cutting velocities, initial sheet temperatures, and punch fillet radii on the directional deformation values of the product.

Cutting velocity

Figure 14 illustrates the relationship between cutting velocity and directional deformation, considering the effects of both initial sheet temperature and punch fillet radius. Figure 14 (a) illustrates the effect of temperature on the deformation values of the product. The deformation is shown to be lowest at 0 °C and increases at 20 °C, 40 °C, 60 °C, and reaches a maximum at 80 °C. As velocity rises from 40 mm/s to 80 mm/s, the deformation rises across all temperature levels. The most significant rise occurs at higher velocities and temperatures, suggesting that the combined effects of elevated temperature and high velocities induce more heat leading to greater material distortion of the copper product. On the other hand, Figure 14 (b) analyzes the effect of fillet radius, where the smallest fillet radius of 0.1 mm results in the least deformation, while the largest fillet radius of 0.9 mm produces the highest deformation. As the fillet radius increases, more material comes into contact with the tool, resulting in higher frictional forces and thus greater deformation, especially at higher velocities.

Both graphs (Figure 14a and 14b) demonstrate that increased temperature and fillet radius, especially at higher velocities, significantly amplify material deformation, highlighting the need to carefully control these parameters to minimize product deformation and maintain product accuracy.

Initial sheet temperature

Figure 15 presents two graphs that depict the relationship between initial sheet temperature and directional deformation, considering the effects of cutting velocity and punch fillet radius on rectangular-shaped product deformation levels. In Figure 15 (a), the effect of velocity is shown across a range of temperatures. As temperature increases from 0 °C to 80 °C, the deformation rises consistently for all velocities. The highest deformation occurs at the velocity of 80 mm/s (red line), while the lowest deformation is observed at the velocity of 40 mm/s (orange line). This demonstrates that higher velocities combined with increasing temperature, significantly increase deformation of the copper product. In Figure 15 (b), the influence of fillet radius is examined over a temperature range

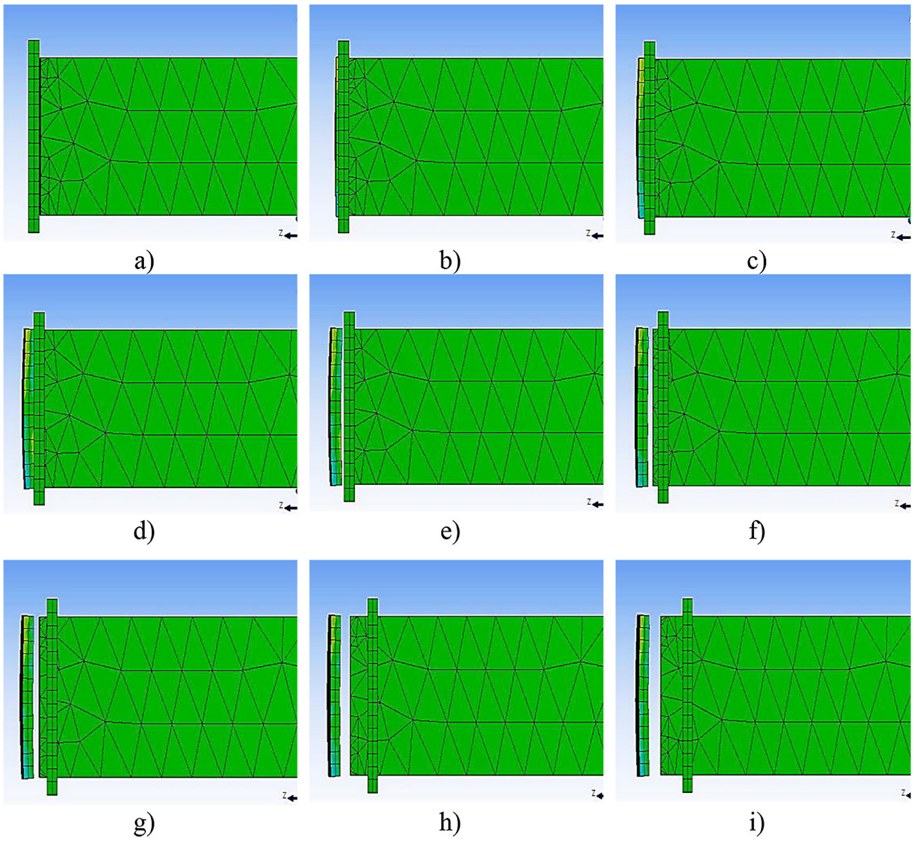

Figure 12. Penetration stages of rectangular-shaped product using a cutting punch

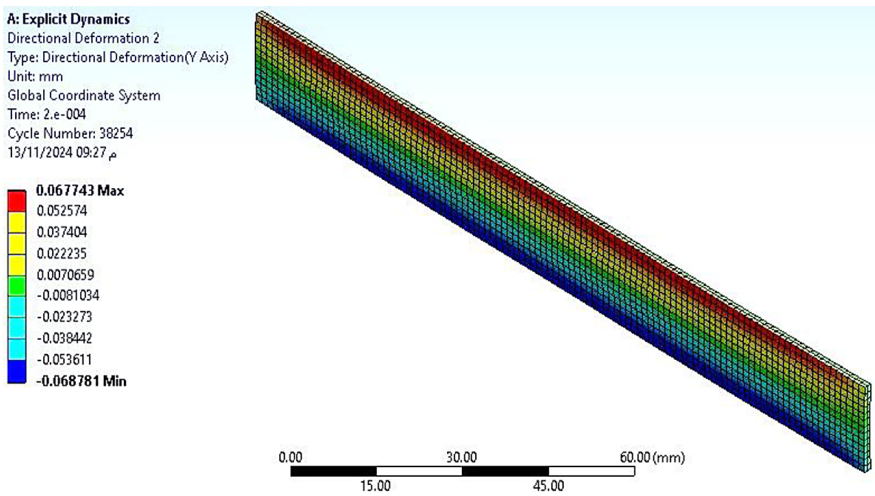

Figure 13. Directional deformations of rectangular shape product

from 30 °C to 90 °C. The smallest fillet radius of 0.1 mm (orange line) produces the least deformation, while the largest fillet radius of 0.9 mm (red line) results in the highest deformation. As temperature increases, the deformations start to grow at the product for all fillet radii, with the effect becoming more prominent at higher radii. This indicates that larger tool geometries, in combination with elevated temperatures, lead to greater material deformation. Both graphs (Figure 15a and 15b) suggest that controlling velocity, temperature, and fillet radius is critical in minimizing deformation, especially in high-temperature conditions where these factors have a compounded effect on metal deformation levels of the rectangular-shaped product.

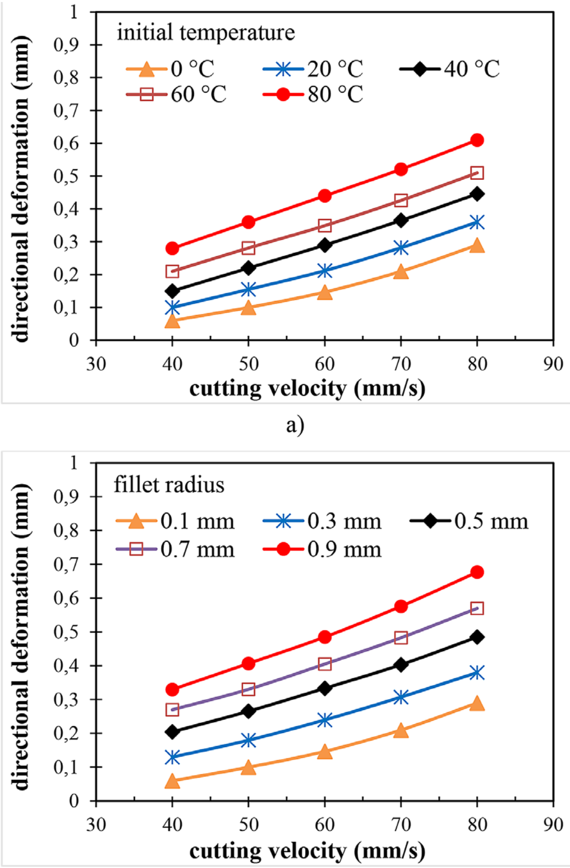

a)

b)

Figure 14. Relation between cutting velocity and deformation at: (a) temperature from 0 to 80 °C and fillet radius of 0.1 mm, (b) fillet radius from 0.1 to 0.9 mm and temperature of 0 °C

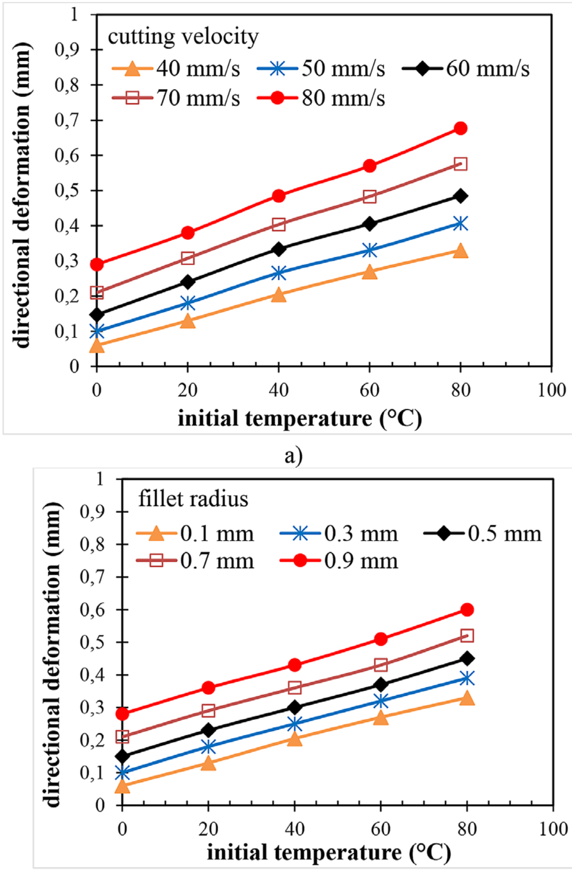

a)

b)

Figure 15. Relation between temperature and deformation at: (a) cutting velocity from 40 to 80 mm/s and fillet radius of 0.1 mm, (b) fillet radius rom 0.1 to 0.9 mm and velocity of 40 mm/s

Punch fillet radius

Figure 16 presents two graphs that depict the relationship between punch fillet radius and directional deformation, considering the effects of initial sheet temperature and cutting velocity on the deformation values of the rectangular shape product. In Figure 16 (a), the influence of temperature is examined across a range of fillet radii. As the fillet radius increases from 0.1 mm to 0.9 mm, deformations increase for all temperature levels. The lowest deformation is observed at 0 °C (orange line), while the highest deformation occurs at 80 °C (red line). The rise in deformation becomes more pronounced at higher fillet radii, indicating that temperature exacerbates material deformation when combined with larger tool geometry. In Figure 16 (b), the effect of velocity is explored over a range of fillet radii. Product deformation increases as both velocity and fillet radius rise. The velocity of 40 mm/s (orange line) produces the least deformation, while the velocity of 80 mm/s (red line) results in the highest deformation. This suggests that higher velocities, in conjunction with larger fillet radii, lead to more substantial metal distortion of the copper product.

Both graphs (Figure 16a and 16b) emphasize that the fillet radius plays a significant role in increasing deformation, especially when combined with elevated temperatures and higher velocities. The results underscore the importance of optimizing these parameters to reduce product deformation and maintain product precision.

Combine cutting velocity and punch fillet radius

The relationship between cutting velocity, punch fillet radius, and directional deformation at an initial sheet temperature of 0 °C is

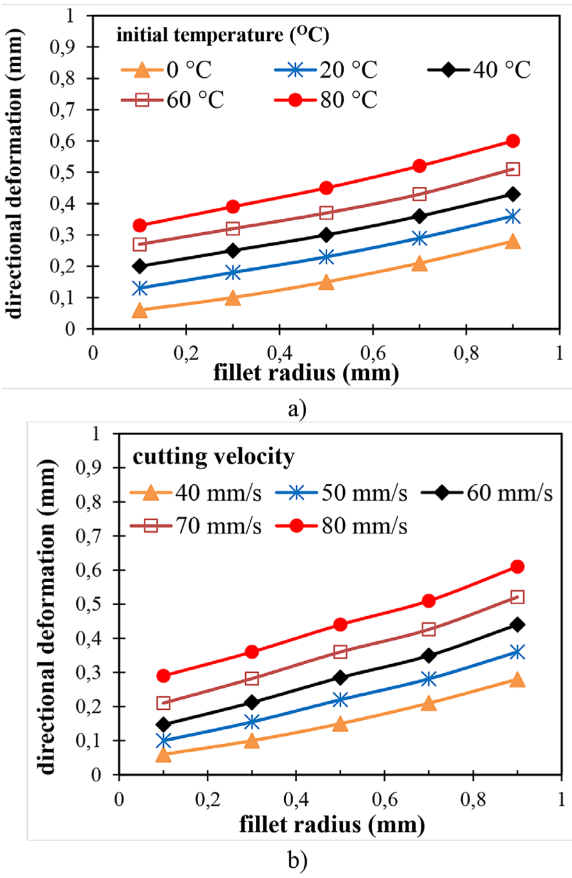

Figure 16. Relation between fillet radius and deformation at: (a) temperature from 0 to 80 °C and cutting velocity of 40 mm/s, (b) velocity from 40 to 80 mm/s and temperature of 0 °C.

presented in the three-dimensional surface plot in Figure 17.

It is shown from the Figure 17 when the values of both velocity and fillet radius increase, the deformation value is raised. In particular, the deformation increases significantly as the velocity rises to the range between 70 and 80 mm/s and fillet radii increase to the range between 0.7–0.9 mm. On the other hand, at a small value of both velocity and fillet radius, the product deformation is at its smaller value. Therefore, the balance between cutting velocity and punch fillet radius is important in improving cutting quality to ensure the accuracy of the product.

Combine cutting velocity and initial sheet temperature

The relationship between cutting velocity, initial sheet temperature, and directional deformation at a fillet radius of 0.1 mm is shown as a three-dimensional surface plot in Figure 18. The figure displays that the product deformation rises when both velocity and temperature increase. More specifically higher velocities (above 60 mm/s) and high temperatures (over 60 °C) result in greater directional deformation because of the raise in friction, heat, and material resistance through the cutting process. Also, it is noticed that the sharp rise in deformation value is more obvious in the high-temperature and high-velocity zones and this leads to yield significant material distortion. On the other hand, metal deformation is reduced when utilizing lower velocities and temperatures. Therefore, balancing the parameters is important to ensure a reduction in product deformation for better surface quality and dimensional accuracy.

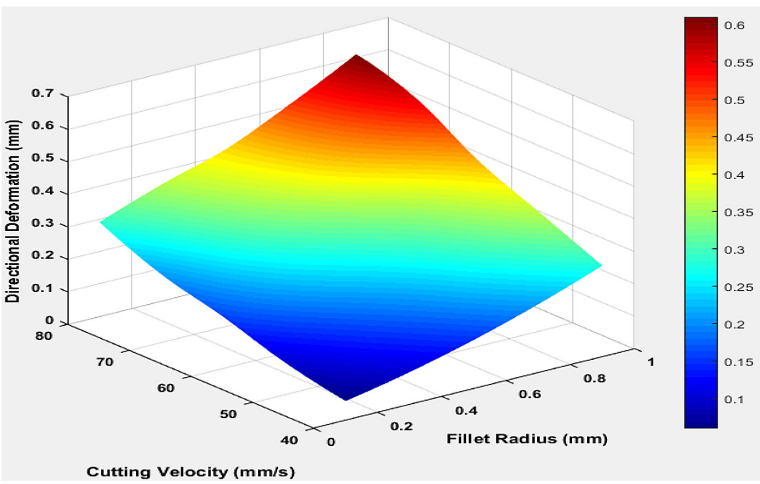

Figure 17. Relation between cutting velocity, punch fillet radius, and directional deformation at initial sheet temperature of 0 °C

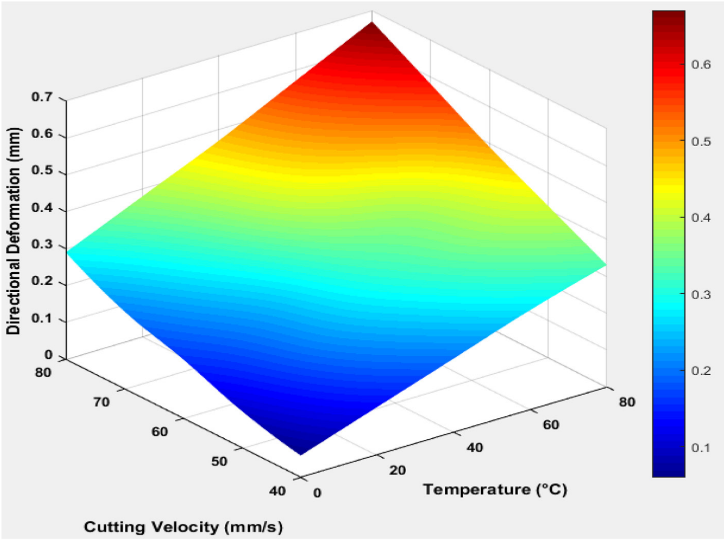

Figure 18. Relation between cutting velocity, initial sheet temperature, and directional deformation at punch fillet radius of 0.1 mm

Combined initial sheet temperature and punch fillet radius

The relationship between initial sheet temperature, punch fillet radius, and directional deformation at a cutting velocity of 40 mm/s is presented in the three-dimensional surface plot in Figure 19. It is shown from the figure that rise the temperature and fillet radius leads to a rise in product deformation. More specifically raising the temperature above 60 °C and fillet radii above 0.7 mm led to a significant raise in the deformation value at the upper-right region of the plot. On the other hand, minimal deformation value accrues at lower temperatures (below 40 °C) and smaller fillet radii (below 0.3 mm). Therefore, moderate temperature and fillet radius values lead to minimum deformation which maintains the structural integrity of the product.

CONCLUSIONS

This study focuses on examining the cutting operation of the rectangular shape oxygen free high conductivity copper sheet to reduce the deformations and achieve a high-quality product. The selected parameters including cutting velocity, initial sheet temperature, and punch fillet radius were investigated in this paper. The overall findings of the current study are:

1. The product deformation was minimal when using a cutting velocity of 40 mm/s, initial sheet temperature of 0 °C, and punch fillet radius of

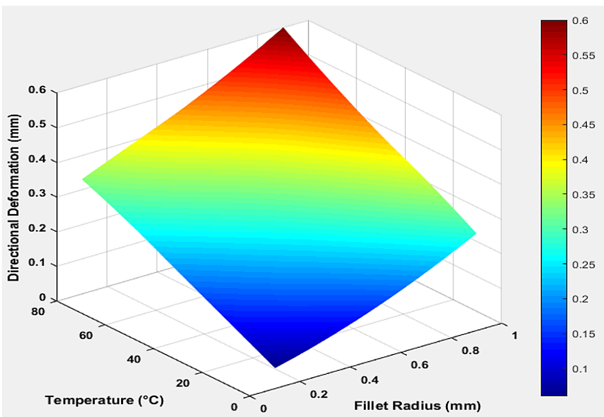

Figure 19. Relation between initial sheet temperature, punch fillet radius, and directional deformation at a cutting velocity of 40 mm/s

0.1 mm. While, it was maximum when using velocity of 80 mm/s, temperature of 80 °C, and fillet radius of 0.9 mm.
2. Raising both cutting velocities (above 60 mm/s) and punch fillet radii (above 0.7 mm) leads to raise in the product deformation by 40%.
3. Increasing the initial sheet temperature (above 60 °C) combined with higher cutting velocity results in a 35% increase in product deformation.
4. Raising the initial sheet temperatures (over 60 °C) and punch fillet radii (bigger than 0.7 mm) lead to a 30% raise in the product deformation.
5. The current study provides better outcomes in terms of directional deformations of the copper product compared with published data using different sheet thicknesses, clearances, and punch wear radii.
6. The cutting mold models with selected parameters can be utilized to manufacture high accuracy copper ruler products under lowest material distortion.
7. The proposed models of cutting molds can provide improved product quality and reduction of manufacturing cost in percentage with accurate dimensions of products.
8. The achieved models of cutting molds can be developed and modified to be used for producing more complicated products and this can lead to potential beneficial to industrial applications in terms of saving time and cost.
9. The current work in terms of cutting mold design procedures and mold models efficiency can contribute to develop the future generation manufacture of products.
10. The current study can be improved by applying some suggestions such as selecting more than three parameters with different values, using high performance computers to save analysis time, choosing complicated products, and conducting experiments.

REFERENCES

1. Kumar K.R., Vettivel S.C., Subramanian R. Mechanical properties and characterization of additively manufactured materials, 1st ed. Florida: CRC Press, 2024. https//doi.org/10.1201/9781003430186
2. Kumar R. Manufacturing process, 1st ed. Kerala: Jyothis Publishers, 2021. Accessed: Sep. 15, 2024. [Online]. Available: https://www.google.iq/books/edition/Manufacturing_Process/NRszEAAAQBAJ?hl=en&gbpv=0&kptab=getbook
3. Katyal K. Essential guide to metals and manufacturing, 1st ed. USA: Xlibris, 2019.Accessed: Sep. 15, 2024. [Online]. Available: https://www.google.iq/books/edition/ Essential_Guide_to_Metals_and_Manufactur/ahKWDwAAQBAJ?hl=en&gbpv=0
4. Awari G.K., Kumbhar V.S., Tirpude R.B., Rajurkar S.W. Automotive manufacturing processes: a case study approach, 1st ed. Florida: CRC Press, 2023. https//doi.org/10.1201/9781003367321
5. Selim, Gurgen, Pruncu C.I. Modern manufacturing processes for aircraft materials, First Edition. Elsevier, 2023. Accessed: Jan. 13, 2025. [Online]. Available: https://www.google.iq/books/edition/Modern_Manufacturing_Processes_for_Aircr/FgimEAAAQBAJ?hl=en&gbpv=0
6. Youssef H.A., El-Hofy H., Ahmed M.H. Manufacturing technology: materials, processes, and equipment, Second Edition. CRC Press, 2024. [Online]. Available: https://www.google.iq/books/edition/Manufacturing_Technology/iUECEQAAQBAJ?hl=en&gbpv=0
7. Dhande U. Handbook of mechanical engineering, Oct. 2024. [Online]. Available: https://www.google.iq/books/edition/Handbook_of_Mechanical_Engineering_Conta/aKQrEQAAQBAJ?hl=en&gbpv=0
8. Tambe L.T., Sadattulla M.U. Mathematical model development & clearance optimization in sheet metal blanking process for copper. International Journal of Progressive Research in Engineering Management and Science, May 2023, 3(5), 460–465.
9. Gökçe H. Modelling and optimization for thrust force, temperature and burr height in drilling of custom 450, Exp Tech, Aug. 2022, 46(4), 707–721, https//doi.org/10.1007/s40799-021-00510-z
10. Badgujar T. Y. and Wani V. P. Prediction of burr height formation in sheet metal trimming processes using acoustic signals and an artificial neural network, International Journal of Mechatronics and Manufacturing Systems, Jul. 2023, 16(1), 22–36, https//doi.org/10.1504/IJMMS.2023.132024
11. Sahli M. et al. Modelling and numerical simulation of steel sheet fine blanking process, in Procedia Manufacturing, Krakow: Elsevier B.V., Sep. 2020, 395–400. https//doi.org/10.1016/j.promfg.2020.08.072
12. Basak S., Kim C., Jeong W., Jung Y. I., and Lee M. G. Numerical prediction of sheared edge profiles in sheet metal trimming using ductile fracture modeling, Int J Mech Sci, Apr. 2022, 219(125), [Online]. Available: https://doi.org/./j.ijmecsci
13. Adnan A. A. K., Azinee S. N., Norsilawati N., and Izzul K. A.M. Analysis of the influence of the

blanking clearance size to the burr development on the sheet of mild steel, brass and aluminium in blanking process, Journal of Achievements in Materials and Manufacturing Engineering, Mar. 2022, 111(1), 26–32, https//doi.org/ 10.5604/01.3001.0015.9093

14. Uzun H., Meral T., and Günay M. Modelling and optimization of burr height in fiber laser drilling of ferritic stainless steel, Manufacturing Technologies and Applications, 2020, 1(2), 32–39.
15. Kolhatkar A. and Pandey A. Experimental and computational investigation of the impact of geometry variation on rollover in sheet metal cutting, in Proceedings of the World Congress on Engineering, London, 2021, 1.
16. Ahmadi F., Abdollahi A., and Zamani S. Experimental study of shearing dimensional parameters in the sheet metal blanking process of StW24 steel with a thickness of 12 mm, Journal of Modern Processes in Manufacturing and Production, 2023, 12(2), 5–21.
17. Mandra A. M., Jiang J., and Xi F. J. A new burr formation model for drilling with tool wear, International Journal of Advanced Manufacturing Technology, Apr. 2021, 116, 1437–1450, https//doi.org/10.1007/s00170-021-07031-4
18. Engin K. E. Finite element analysis of notch depth and angle in notch shear cutting of stainless-steel sheet, Journal of Mechanical Engineering, 2023, 69(7–8), 326–338.
19. Wu F., Liu Z., Guo B., Sun Y., and Chen J. Research on the burr-free interrupted cutting model of metals, J Mater Process Technol, Sep. 2021, 295, 1–8.
20. Yousefi M. and Pervaiz S. 3D finite element modeling of wear effects in the punching process,” Simul Model Pract Theory, Jan. 2022, 114, 1–8.
21. Shaheen W., Kanapathipillai S., Mathew P., and Prusty G. Optimization of compound die piercing punches and double cutting process parameters using finite element analysis, Journal of Engineering Manufacture, 2020, 234, 1–2, 3–13.
22. Takalkar A. S. and Chinnapandi L. B. M. Electro-thermo-mechanical FE simulations of OFHC Cu material for electric contact with DC/AC currents, in 2016 Int. Conf. on Advances in Computing, Communications and Informatics (ICACCI), Jaipur: IEEE, Nov. 2016, 2131–2137. https//doi.org/10.1109/ICACCI.2016.773236
23. Salman M., Guski V., and Schmauder S. Two-scale modeling of nano-clay-filled shape memory polymers, J Micromech Mol Phys, 2022, 7(2), 71–80.
24. Amazon, “Copper Ruler,” Amazon Canada. Accessed: Apr. 10, 2024. [Online]. Available: https://www.amazon.ca/Scissors-Thickened-Straight-Accessory-Thickness/dp/B0CCSRMFX8
25. MatWeb, Oxygen-Free High Conductivity Copper, Hard, UNS C10200, MatWeb Company. Accessed: Apr. 15, 2024. [Online]. Available: https://www.matweb.com/search/DataSheet.aspx?MatGUID=0db21ddedce14e16993ee5cbdf97878d&ckck=1
26. Suchy I. Handbook of Die Design, 2nd ed. USA: McGraw-Hill, 2006. https//doi.org/10.1036/0071462716
27. Boljanovic V. Sheet Metal Forming Processes and Die Design, 4th ed. New York: Industrial Press Incorporated, 2021. Accessed: Apr. 20, 2024. [Online]. Available: https://www.google.iq/books/edition/_/1XPl0AEACAAJ?hl=en&sa=X&ved=2ahUKEwjDw9n7npGJAxWjSfEDHQTWO2AQ7_IDegQIExAD
28. Jain K. C. and Chitale A. K. Textbook of Production Engineering, 2nd ed. India: PHI Learning, 2014. Accessed: Apr. 20, 2024. [Online]. Available: https://www.google.iq/books/edition/TEXTBOOK_OF_PRODUCTION_ENGINEERING/NYxeBAAAQBAJ?hl=en
29. Groover M. P. Fundamentals of Modern Manufacturing: Materials, Processes, and Systems, 7th ed. John Wiley & Sons, 2021. Accessed: Apr. 25, 2024. [Online]. Available: https://www.google.iq/books/edition/Fundamentals_of_Modern_Manufacturing/FuK1EAAAQBAJ?hl=en&gbpv=0
30. Venkataraman K. Design of Jigs, Fixtures and Press Tools, 2nd ed. India: Springer International Publishing, 2022. https//doi.org/10.1007/9783030765330
31. Benck R. F., Franz R. E., and Diberardo D. A. Quasi-Static Stress-Strain Curves, S-7 Tool Steel, Technical Report, Ballistic Research Laboratory, Maryland, 1980. Available: https://apps.dtic.mil/sti/tr/pdf/ADA093773.pdf
32. Govindan K., Kumar H., Yadav S. Advances in Mechanical and Materials Technology. Springer, 2022.
33. Satoba V. S. and Vilas S. B. An overview of effect of punch tool wear radius on burr formation in sheet metal blanking, International Journal of Modern Engineering Research, 2016, 6,(1), 6–11, [Online]. Available: www.ijmer.com